The Journal of Chemical Physics

RESEARCH ARTICLE | APRIL 01 2025

# Exploring superconductivity under strong coupling with the vacuum electromagnetic field

**Special Collection:** Polaritonics for Next Generation Materials

A. Thomas ; E. Devaux ; K. Nagarajan ; T. Chervy ; M. Seidel ; G. Rogez ; J. Robert ; M. Drillon; T. T. Ruan; S. Schlittenhardt; M. Ruben ; D. Hagenmüller ; S. Schütz; J. Schachenmayer ; C. Genet; G. Pupillo ; T. W. Ebbesen



*J. Chem. Phys.* 162, 134701 (2025)
https://doi.org/10.1063/5.0231202

The Journal of Chemical Physics ARTICLE pubs.aip.org/aip/jcp

# Exploring superconductivity under strong coupling with the vacuum electromagnetic field

Cite as: J. Chem. Phys. 162, 134701 (2025); doi: 10.1063/5.0231202
Submitted: 29 July 2024 • Accepted: 12 January 2025 •
Published Online: 1 April 2025



A. Thomas,[1,a] E. Devaux,[1] K. Nagarajan,[1,b] T. Chervy,[1,c] M. Seidel,[1,d] G. Rogez,[2] J. Robert,[2] M. Drillon,[2] T. T. Ruan,[3] S. Schlittenhardt,[3] M. Ruben,[1,3] D. Hagenmüller,[1] S. Schütz,[1] J. Schachenmayer,[1] C. Genet,[1] G. Pupillo,[1,e] and T. W. Ebbesen[1,e]

## AFFILIATIONS

[1] University of Strasbourg and CNRS, ISIS & CESQ, 67000 Strasbourg, France
[2] University of Strasbourg and CNRS, IPCMS, 67000 Strasbourg, France
[3] Karlsruhe Institute of Technology, Institute of Nanotechnology, 76344 Eggenstein-Leopoldshafen, Germany

**Note:** This paper is part of the JCP Special Topic on Polaritonics for Next Generation Materials.
[a] **Current address:** IISc, Department of Inorganic and Physical Chemistry, Bengaluru, India.
[b] **Current address:** TIFR, Department of Chemical Sciences, Mumbai, India.
[c] **Current address:** NTT Research, PHI Labs, Sunnyvale, California 94085, USA.
[d] **Current address:** DESY, Hamburg, Germany.
[e] **Authors to whom correspondence should be addressed:** pupillo@unistra.fr and ebbesen@unistra.fr

## ABSTRACT

Strong light–matter interactions have generated considerable interest as a means to manipulate material properties. Here, we explore this possibility with the molecular superconductor $Rb_3C_{60}$ under vibrational strong coupling (VSC) to surface plasmon polaritons. By placing the superconductor-surface plasmon system in a SQUID magnetometer, we find that the superconducting transition temperature ($T_c$) increases from 30 to 45 K at normal pressures under VSC, displaying a well-defined Meissner effect. A simple theoretical framework is provided to understand these results based on an enhancement of the electron–phonon coupling. This proof-of-principle study opens a new tool box to not only modify superconducting materials but also to understand the mechanistic details of different superconductors.



## I. INTRODUCTION

Over the past 15 years, light–matter strong coupling has emerged as a powerful means to manipulate material properties.[1–33] Light–matter strong coupling is typically achieved by placing a material in a resonant Fabry–Perot cavity or in the confined electromagnetic field of a surface plasmon polariton (SPP) mode. Strong coupling leads to the formation of hybrid light–matter polaritonic states separated by a Rabi splitting. Even in the dark, this Rabi splitting has a finite value due to the vacuum electromagnetic field and can be collectively enhanced with the number of coupled oscillators in the material. It is possible to couple both the electronic and vibrational transitions of a material. Electronic strong coupling (ESC) has been shown to modify chemical reactivity and material properties and leads to an enhancement of charge and energy transport.[4–12,30] The strong coupling of molecular vibrations (VSC) can also induce remarkable changes in chemical reactivity landscapes,[21–24,26–29] and transport properties such as conductivity and ferromagnetism.[16,25,31] In a separate study, we have shown that the weak ferromagnetism of $YBa_2Cu_3O_{6+\delta}$ nanoparticles due to unpaired lattice vacancies can be enhanced by a factor 700 under VSC, depressing the natural $T_c$ of the material due to the high magnetic field.[16] Theoretical studies predict that strong coupling could possibly change the $T_c$ of superconductors.[14,32–34] We have extensively studied the superconductor $Rb_3C_{60}$ under VSC. Despite experimental difficulties, as explained further in the following, the statistics indicate that 70% of the samples show an increase in $T_c$ centered at 45 K compared to a transition at 30 K under normal conditions.

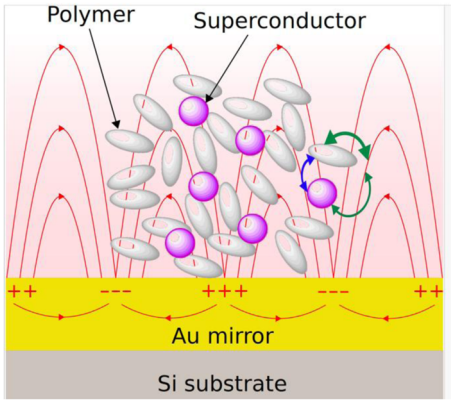


**FIG. 1.** Sketch of the experimental sample where superconductor grains (average size ~200 nm) are embedded in a polymer film (thickness ~4.5 $\mu$m) and deposited on a metal layer (Au, thickness 20 nm). The metal–dielectric interface generates surface plasmon polaritons (SPPs) with electric field represented by the thin red lines.

$Rb_3C_{60}$ is a strongly correlated material where superconductivity is understood to be phonon-mediated.[35,36] The challenge in coupling phonons in these compounds to the vacuum field stems from their weak transition dipole moments, which prevent reaching the strong coupling regime. As we have shown elsewhere,[16,19,20] it is nevertheless possible to reach this regime by exploiting a vibrational environment consisting of auxiliary oscillators that are strongly coupled to cavity photons, and resonant with the target oscillators. As illustrated in Fig. 1, for this purpose, the $Rb_3C_{60}$ superconductor powder is blended with a polymer, polystyrene (PS), which has a vibrational transition that is resonant with the phonon mode of the superconductor. The polymer is strongly coupled to the surface plasmons and in turn induces what is known as cooperative strong coupling in the superconductor. In other words, the vacuum field dresses the weak phonon modes of $Rb_3C_{60}$ through cooperative strong coupling[16,19,20] of the PS vibrational mode.

## II. EXPERIMENTAL METHODS

All the glassware (NMR tubes, vials, pipettes, and micropipettes) used for the preparation of the $Rb_3C_{60}$ powder were carefully cleaned and baked at 450°, before being introduced in the glovebox. We then waited 24 h before preparing the superconducting powder. $C_{60}$ was weighed and introduced in an NMR tube and then Rb was taken with a micropipette from an ampule and added to the $C_{60}$ powder inside the glovebox. Knowing the diameter of the micropipette and measuring the length filled with Rb, one is able to estimate the Rb weight and thus the ratio Rb/$C_{60}$ in molar units, which was kept between 3 and 5. We found that a too large excess of Rb (ratio >5) was detrimental to obtain superconducting material. After that, the tube was closed with a stopcock, taken out of the glovebox and plugged onto a Schlenk line, pumped before being sealed by melting the tube with a small gas torch. The last step was to place this tube containing the $C_{60}$ and Rb mixture in an oven at 390° for 72 h. The obtained $Rb_3C_{60}$ (black powder) was then characterized by SQUID magnetometry to check its properties ($T_c$ and moment). When the measured ZFC moment was lower than 0.003, meaning a very low superconducting fraction, the powder was not used to prepare films for strong coupling.

We produced 55 batches of $Rb_3C_{60}$ powder. The superconducting fraction varied from sample to sample and estimated to be between ~0.5%–8%. The superconducting fraction is of course hard to estimate due to different parameters (in particular, because of the powder nature of our samples) and might have been underestimated.[37] What we have noticed is that the measured magnetic moment from which this fraction was estimated was varying by upto 2 orders of magnitude over all our trials. $T_c$ itself was not always exactly the same being 30 ± 2 K. Furthermore, the SQUID magnetometry measurements were performed in different places with four different machines [Quantum Design facility (Darmstadt), ISIS and IPCMS (Strasbourg), and KIT (Karlsruhe)] for both the initial $Rb_3C_{60}$ powder and the final films, prepared as explained next.

After the $Rb_3C_{60}$ synthesis, the NMR tubes containing the superconducting material were placed in the glovebox, opened and the $Rb_3C_{60}$ powder was ground in a (clean and baked) mortar. After grinding, half of the powder was always kept in a separate tube to check its $T_c$ to control that it had not changed, whereas the second half was mixed in a PS toluene solution to be spin coated on Si substrates or Au coated Si substrates. Before that, the Si substrates were cleaned in successive baths of acetone and isopropanol in a sonicator (ultrasound cleaner) and then rinsed with ultrapure water before being introduced in the glovebox 24 h before use. In addition, toluene was distilled and purged for one hour with Ar and sealed with a septum before its introduction into the glovebox together with the polystyrene. The PS concentration in toluene was 14% in weight and the $Rb_3C_{60}$ concentration 6% in weight of the polymer solution. With this concentration, we obtained ~4.5 $\mu$m thick films on Si or Au coated Si substrates when spin-coated at 1000 rpm. A higher concentration of $Rb_3C_{60}$ increases the scattering and was detrimental for strong coupling. Then, those substrates were cut in small rectangular pieces of ~3 × 5 $mm^2$ and 3 of those were then placed at the bottom of an NMR tube. To take out the samples from the glovebox, we used the same procedure as described above, with a stopcock to close the NMR tube containing the samples. The tube was immediately sealed on the Schlenk line to minimize any possible $O_2$ contamination. The weight of superconducting powder into the samples was estimated by weighing substrates before and after spin-coating of the powder in polymer solution, taking into account the further cutting of the substrate in small pieces. We obtained a rough estimation of 0.07 mg of powder per tube. Given this tiny amount and the varying superconducting fraction from one powder batch to another, one can easily understand that the results can only be statistical.

## III. EXPERIMENTAL RESULTS

The influence of strong coupling on the superconducting transition of $Rb_3C_{60}$ was investigated using this approach. We chose SPPs as optical modes since the use of a resonant Fabry–Perot cavity would have been complicated by the change of the cavity path length at low temperature during SQUID magnetometry measurements. Since the cavity resonances are highly sensitive to the path length, the changes to the latter can tune/detune the cavity mode from the PS/$Rb_3C_{60}$ resonance. Fullerene superconductors are extremely air and humidity sensitive due to the triple radical nature of the reduced

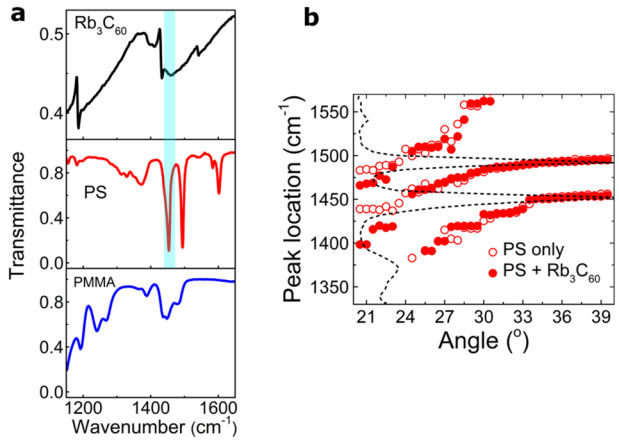


**FIG. 2.** (a) FTIR spectrum of $Rb_3C_{60}$ powder (top), PS (middle), and PMMA (bottom). The overlapping of the Ag pinch mode at 1454 $cm^{-1}$ with the PS vibrational mode is highlighted in cyan. (b) Polariton dispersion curves showing strong coupling of the PS (empty circles) and $Rb_3C_{60}$ + PS (solid circles) films on Au. The Rabi splitting between the first two polariton branches is 32 $cm^{-1}$.

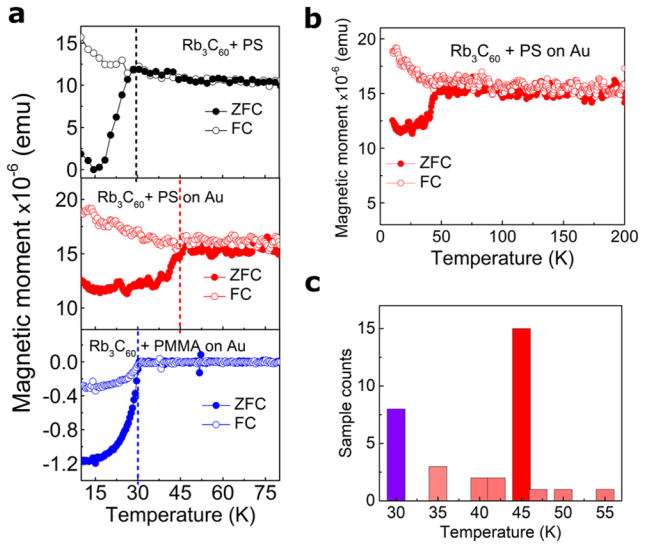


**FIG. 3.** (a) Magnetization curves in the ZFC and 100 Oe FC modes of the bare film of $Rb_3C_{60}$ + PS on Si (top), strongly coupled $Rb_3C_{60}$ + PS on Au (middle), and cooperatively off-resonant $Rb_3C_{60}$ + PMMA on Au (bottom). For both the bare film and cooperatively off-resonant $Rb_3C_{60}$ film, the $T_c$ is at 30 K, while it is increased to 45 K for the strongly coupled $Rb_3C_{60}$ film, as indicated by the dashed lines. The magnetization offsets are attributed to the substrates and the Pyrex tube (see the supplementary material). (b) Details of magnetization of a strongly coupled $Rb_3C_{60}$ film ($Rb_3C_{60}$ + PS on Au). (c) The statistics of the observed $T_c$ for the various $Rb_3C_{60}$ + PS on Au samples studied showing a maximum at 45 K (red bar).

$C_{60}$, so special precautions had to be taken in the preparation of the samples (see Sec. II).

The IR spectrum of $Rb_3C_{60}$ is shown in Fig. 2(a) with a weak but distinct peak at 1454 $cm^{-1}$. This is one of the Raman-active on-ball modes of $C_{60}$ (Ag pinch mode) that is also IR active due to a symmetry breaking stemming from the coupling to electronic transitions in the presence of disorder.[38,39] This mode is thought to play an important role in the Cooper pairing mechanism due to a large electron–phonon coupling.[36] To achieve cooperative coupling with this mode, we chose to disperse the superconductor in PS, which features a matching vibrational band. Since it is not possible to prepare an off-resonance condition with PS, we also used another polymer polymethylmethacrylate (PMMA) as a control, where the PMMA vibrational mode is too broad to reach the strong coupling condition at 1450 $cm^{-1}$ region, as discussed next.

Since the use of a resonant Fabry–Perot cavity is made difficult by the change of the cavity path length at low temperature, we chose to spin-coat the $Rb_3C_{60}$ + polymer mixture onto an Au layer to couple to SPPs. The plasmonic substrate used in our experiments, shown schematically in Fig. 1, will be inefficient in supporting any Tamm plasmon modes as there is only a single Au–Si interface and no Au-DBR (distributed Bragg reflector).[40] The polariton dispersion curves of the samples were measured by attenuated total reflection (ATR) using an FTIR (Fourier transform infrared) spectrophotometer, and these are shown in Fig. 2(b). Strong coupling of the PS mode at 1454 $cm^{-1}$ yields a Rabi splitting of 32 $cm^{-1}$, larger than the FWHM of this mode (10 $cm^{-1}$). The dispersion of the PS film on Au displays anti-crossings when the two vibrational modes of PS are in resonance with SPPs. $Rb_3C_{60}$ phonons do not contribute directly to strong coupling since the dispersion curves of $Rb_3C_{60}$ + PS on Au are practically identical to that of PS on Au.

For superconductivity measurements, the $Rb_3C_{60}$ samples spin-casted on Au-coated Si were then cut into small strips (~3 × 5 $mm^2$) placed in sealed Pyrex (or quartz) tubes, introduced into the SQUID magnetometer (either a MPMS or a MPMS3, "Quantum Design Europe"). SQUID magnetometry is a well-established technique to characterize the Meissner effect, which is one of the two hallmarks of superconductivity together with a zero electrical resistance. The Meissner effect is demonstrated by measuring both the field-cooled (FC) and zero-field-cooled (ZFC) magnetization curves. Here, the latter are typically recorded between room temperature and 4 K at 100 Oe and are shown in Fig. 3. The Meissner effect is clearly visible in Figs. 3(a) and 3(b), the PS + $Rb_3C_{60}$ film on Au shows a $T_c$ of 45 K (50% increase over the normal $T_c$ of 30 K), which is even larger than the $T_c$ of fullerides (38 K) measured for $Cs_3C_{60}$ under high pressure.[41] Our optimized protocol yielded a $T_c$ of 45 K for most of the PS + $Rb_3C_{60}$ samples under VSC with some outliers, as shown in Fig. 3(c). Out of the 33 samples tested, some remained at 30 K, which, by inspection, we attribute to delamination of the polymer film from the Au substrate during cooling. When the polymer layer is detached from the Au surface, strong coupling no longer occurs, and as a result, the $T_c$ remains at 30 K.

The optimal loading of $Rb_3C_{60}$ in the polymer was found to be around 6 wt. %. Since $Rb_3C_{60}$ is not soluble in toluene, we observed that a higher loading of the superconductor leads to increased scattering and reduces the strong coupling effect, as mentioned earlier. We emphasize that the existence of a single drop in the magnetization curves of Fig. 3 indicates that the entire superconducting volume fraction in the sample features a modified $T_c$ in the presence of cooperative strong coupling. In a few samples (Fig. S7),

we observed a drop at 30 K, indicating a fraction of uncoupled $Rb_3C_{60}$, which could be due to the onset of delamination, orientation effects, or variation of electric field intensity across the sample. When PMMA is the host polymer on Au [Fig. 3(a) bottom panel and Fig. S9] and in the absence of the Au film, Fig. 3(a) and Fig. S8, no change in $T_c$ is observed. The control samples of PMMA + $Rb_3C_{60}$ have no effect on $T_c$ because the oscillator strength of PMMA vibrational bands overlapping with the superconductor is too small to lead to strong coupling (see Figs. S9 and S10). We characterized the $T_c$ of only two PMMA + $Rb_3C_{60}$ samples, as there is no cooperative VSC between PMMA and $Rb_3C_{60}$. The increase in $T_c$ of PS + $Rb_3C_{60}$ contrasts the reduction to $T_c$ observed for PS + $YBa_2Cu_3O_{6+\delta}$ nanoparticles due to 700-fold enhancement in the ferromagnetism under VSC.[16] Again, there is no change of either $T_c$ or ferromagnetism in PMMA + $YBa_2Cu_3O_{6+\delta}$ nanoparticles, as there is no VSC.[16] The latter also acts as a control experiment for the PS + $Rb_3C_{60}$ and shows that the PS or PMMA as a polymer matrix alone in the absence of VSC has no role in the enhanced $T_c$ of $Rb_3C_{60}$. Hence, the change in $T_c$ is not some spurious effect due to the protocol and cannot be due to the presence of oxygen since it would be everywhere and would not lead to a Meissner effect, which is an absolute proof of a superconducting transition. In view of the very small quantities of $Rb_3C_{60}$, the magnetization moments are only $10^{-6}$ emu, which explains the noisiness of the data, as shown in the supplementary material Fig. S7, and the need to make a statistical ensemble of samples as we did. Another challenge that we found was preparing a superconductive $Rb_3C_{60}$ with a large superconductive fraction, a well-known problem due among other things to the different crystalline phases and the different stoichiometries that co-exist in such molecular samples.[37,39]

## IV. THEORETICAL RESULTS

We now introduce a theoretical model providing a qualitative explanation for the observed enhancement of $T_c$ in $Rb_3C_{60}$ due to cooperative strong coupling between SC phonons and SPPs. In conventional SCs, such as $Rb_3C_{60}$,[42] $T_c$ increases with the strength of the electron–phonon interaction, which governs the scattering of electrons across the Fermi surface giving rise to Cooper pairing.[42] These processes are usually quantified by the dimensionless parameter $\lambda$.[43,44]

For a spherical Fermi surface and an optical phonon mode with frequency $\omega_q$, the parameter $\lambda \propto \int_0^{2k_F} dqqV_q/\omega_q$, where $q$ is the phonon wave vector, $k_F$ is the Fermi wave vector, and $V_q$ is the electron–phonon coupling matrix element. For large light–matter couplings, one could in principle exploit the formation of low frequency polaritonic states to effectively reduce $\omega_q$, which would lead to an enhancement of $\lambda$. However, sizable shifts of $\omega_q$ are usually hampered by the small coupling strength of SC phonons to the vacuum electromagnetic field.[14,45] Furthermore, while the largest shifts occur close to the resonance at optical wave-vectors $q \sim \omega_q/c \ll k_F$ ($c$ is the speed of light), $V_q$ is in general a slowly varying function of $q$,[46] which implies that large enhancements of $\lambda$ can be mainly engineered by a reduction of $\omega_q$ at large wave-vectors $q \sim k_F$.

Here, we propose a mechanism to induce large phonon shifts at wave vectors $q \sim k_F$ relevant for superconductivity via the auxiliary polymer. When the polymer and the SC phonons are quasi-resonant, we find that a strong coupling of the polymer to the far off-resonant electromagnetic field for which $q \sim k_F \gg \omega_q/c$ leads to a low-frequency polariton containing a finite SC phonon weight due to direct dipole–dipole interactions of the latter with the polymer. This results in an enhancement of $\lambda$ that increases with the polymer coupling strength to SPPs.

The film is described as an effective homogeneous dielectric medium with background dielectric constant of the polymer $\varepsilon$, and two optical phonons with bare frequencies $\omega_{sc}$ and $\omega_{ps}$, associated to an on-ball mode of $C_{60}$ and the quasi-resonant mode of PS, respectively. Dipole–dipole self-interactions for each type of phonons provide a depolarization shift of the bare frequencies: $\tilde{\omega}_{SC} = \sqrt{\omega_{sc}^2 + \nu_{sc}^2 f}$ and $\tilde{\omega}_{ps} = \sqrt{\omega_{ps}^2 + \nu_{ps}^2(1-f)}$, where $f$ is the SC volume fraction in the film (loading) and $\nu_{sc/ps}$ are associated to the phonon oscillator strengths. These shifted frequencies correspond to the minima of a transmission spectrum measured at normal incidence (top of the polariton gaps[47]). The two types of phonons further interact with each other via direct dipole–dipole coupling with strength $\Lambda^{sc-ps} \propto \nu_{sc}\nu_{ps}\sqrt{f(1-f)}$. Photons are coupled to SC and PS phonons with strengths $\Omega_{q_\parallel}^{sc-pt} \propto \nu_{sc}\sqrt{f}$ and $\Omega_{q_\parallel}^{ps-pt} \propto \nu_{ps}\sqrt{1-f}$, respectively, and to plasmons in the metal (plasma frequency $\omega_{pl}$) with strength $\Omega_{q_\parallel}^{pl-pt} \propto \sqrt{\omega_{pl}}$ [Fig. 4(a)]. All the modes coupled to light are quasi-2d "bright" modes with a given in-plane wave vector $q_\parallel$ (parallel to the metal–dielectric interface), superpositions of the 3d modes with different wave vectors in the out-of-plane direction. The resulting Hamiltonian comprises four coupled harmonic oscillators (see the supplementary material), whose eigenvalues provide the polariton spectrum shown in Fig. 4(b). At large wave vectors $q_\parallel \sim 2k_F$, the spectrum consists of a light mode (P4) with $\omega \sim cq_\parallel\sqrt{(1+\varepsilon)/\varepsilon}$, a SPP mode (P3) with $\omega \sim \omega_{pl}/\sqrt{1+\varepsilon}$, and two "dressed" phonons (P1, P2) at much lower frequencies.

We find that the electron–phonon coupling parameter $\lambda$ is enhanced by the formation of the lowest polariton P1. Motivated by the dispersion curves (see the supplementary material), we assume $\nu_{ps} > \nu_{sc}$. For small $f$, the collective dipole moment of PS phonons $\nu_{ps}\sqrt{1-f}$ thus largely exceeds that of the SC phonons $\nu_{sc}\sqrt{f}$, and the light–matter coupling is dominated by the polymer. In this case, the frequency of P1 at large $q_\parallel \sim 2k_F$ is close to the bottom of the PS polariton gap, $\omega_{ps}$, just as in polar crystals where the lower phonon polariton approaches the transverse optical phonon frequency at large wave vectors. Furthermore, when the two shifted phonons are in resonance ($\tilde{\omega}_{sc} = \tilde{\omega}_{ps}$), the PS phonon frequency $\omega_{ps}$ lies below $\omega_{sc}$, i.e., $\delta \equiv \omega_{ps} - \omega_{sc} < 0$ [see Fig. 4(c)], and one obtains an effective redshift of SC phonons at large wave vectors if P1 contains a significant SC phonon weight. The latter is achieved via the hybridization of SC and PS phonons due to direct dipole–dipole interactions, which is maximum (50%–50%) when $\tilde{\omega}_{sc} = \tilde{\omega}_{ps}$. We expect that this latter resonance condition is relaxed in the experiments due to the finite phonon linewidth that is not included in the model. Figure 3(d) shows the relative change $\Delta\lambda/\lambda_0 \equiv (\lambda - \lambda_0)/\lambda_0$ as a function of detuning $\delta$, $f$, and $\nu_{ps}$, with $\lambda_0$ being the bare electron–phonon coupling parameter ($\nu_{sc} = \nu_{ps} = 0$). We find that the enhancement of the coupling parameter $\lambda$ for $\delta < 0$ strongly

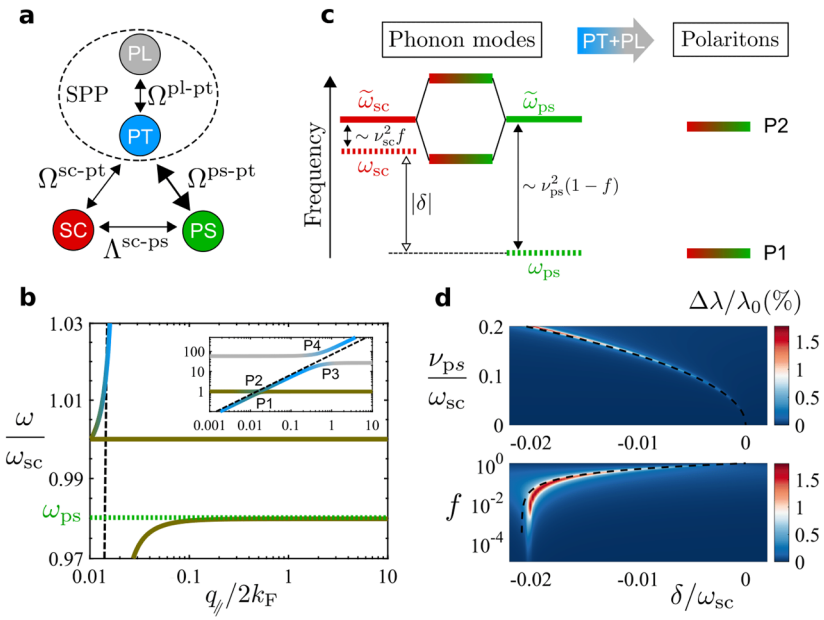


**FIG. 4.** Theoretical model. (a) Sketch of the four relevant bosonic modes of the model and their coupling strengths: SC (red) and PS (green) phonons are coupled among each other and to photons (PT), which are hybridized with plasmons (PL) to SPPs (dashed circle). (b) Polariton energy dispersion ($f = 0.02$, $\nu_{ps} = 0.2\omega_{sc}$, and $\delta \approx -0.02\omega_{sc}$) with mode admixtures (line colors correspond to a). The brownish color of P1 indicates a mixture of SC and PS with a SC phonon weight 49.6% for $q_{\parallel} = 2k_F$. The photon dispersion $\omega \sim q_{\parallel}c/\sqrt{\varepsilon}$ is depicted by the black dashed line. (c) Sketch of the energy levels for $q_{\parallel} \sim k_F$, including energy shifts of phonons due to dipolar self-interactions ($\omega_{sc/ps} \to \tilde{\omega}_{sc/ps}$). Enhancement of $\lambda$ can be achieved for a P1 with frequency smaller than $\omega_{sc}$ ($\delta \equiv \omega_{ps} - \omega_{sc} < 0$) and substantial SC weight ensured by $\tilde{\omega}_{sc} = \tilde{\omega}_{ps}$. This can occur when the collective dipole moment of PS phonons $\nu_{ps}\sqrt{1-f}$ exceeds that of SC phonons $\nu_{sc}\sqrt{f}$. (d) $\Delta\lambda/\lambda_0$ (%) vs $\delta$, $\nu_{ps}$, and $f$, for $f = 0.02$ (top) and $\nu_{ps} = 0.2\omega_{sc}$ (bottom). The dashed lines correspond to $\tilde{\omega}_{sc} = \tilde{\omega}_{ps}$.

increases with $\nu_{ps}$ and features a maximum at small SC concentration $f \sim 0.01$ in qualitative agreement with the experiments. While our model is too simple to be used to directly predict $T_c$, which also depends on, e.g., the averaged SC phonon frequencies,[43,44] it shows that $\lambda$ can be significantly modified by interactions with a strongly coupled polymer.

## V. CONCLUSION

While more experiments are clearly needed, the results show unambiguously than one can modify the $T_c$ of the molecular $Rb_3C_{60}$ superconductor by strongly coupling one of its phonon modes. An alternative to SPPs coupling could be to use the cavities with fixed spacing and materials with much smaller thermal expansion coefficients. One could also imagine to find a more stable type I superconductor to facilitate such investigations, that were made difficult here by experimental constraints due to the oxidation sensitivity of the compound. Coupling superconductors in the THz frequency range may also facilitate the expansion of the potential range of materials. Finally, VSC has already proven to be a powerful tool to modify matter properties, particularly in chemistry, and our results show that it might also be an elegant way to increase $T_c$ of superconductors, without the need for ultrahigh pressures or short pulse lasers.[48,49]

## SUPPLEMENTARY MATERIAL

The supplementary material provides additional temperature-dependent magnetization curves of 24 different samples, FTIR spectra, dispersion curves, and SEM images. In addition, the extended theoretical analysis is presented.

## ACKNOWLEDGMENTS

The authors acknowledge support from the International Center for Frontier Research in Chemistry (icFRC, Strasbourg), the ANR EquipexUnion (Grant No. ANR-10-EQPX-52-01), the Labex NIE projects (Grant No. ANR-11-LABX-0058NIE) and the CSC (Grant No. ANR-10-LABX-0026CSC) within the "Investissement d'Avenir" Program No. ANR-10-IDEX-0002-02, the ERC (Project No. 788482 MOLUSC), and the ANR ERA-NET QuantERA project "RouTe" (Grant No. ANR-18-QUAN-0005-01). M.S. acknowledges funding from the European Union's Horizon2020 programme under the Marie Skłodowska-Curie Grant Agreement No. 753228. G.P. acknowledges additional support from the "Institut Universitaire de France" (IUF) and the University of Strasbourg Institute for Advanced Studies (USIAS). D.H. thanks Y. Laplace for valuable discussions. The authors thank T. Adler and S. Riesner from "Quantum Design Europe" for measurements in Darmstadt and the assistance of the following people: B. Lainer, M. Piejko, S. Kushida, A. Jayachandran, and B. Patrahau.

## AUTHOR DECLARATIONS

### Conflict of Interest

The authors have no conflicts to disclose.

### Author Contributions

T.W.E. initiated the study and oversaw the experiments. Experiments were performed by A.T., E.D., K.N., T.C., M.S., G.R., J.R. T.T.R, and S.S. Theoretical investigations were led by D.H. and G.P. and conducted by D.H., S.S., J.S., and G.P. The manuscript was written by A.T., D.H., S.S., J.S., G.P., and T.W.E.; all authors discussed the results and contributed to the manuscript.

**A. Thomas**: Data curation (equal); Formal analysis (equal); Investigation (equal); Validation (equal); Writing – original draft (equal); Writing – review & editing (equal). **E. Devaux**: Data curation (equal); Formal analysis (equal); Investigation (equal); Writing – original draft (equal); Writing – review & editing (equal). **K. Nagarajan**: Investigation (equal); Validation (equal); Writing – review & editing (equal). **T. Chervy**: Data curation (equal); Formal analysis (equal); Investigation (equal); Writing – review & editing (equal). **M. Seidel**: Data curation (equal); Investigation (equal); Writing – review & editing (equal). **G. Rogez**: Data curation (equal); Formal analysis (equal); Investigation (equal); Validation (equal); Writing – review & editing (equal). **J. Robert**: Data curation (equal); Formal analysis (equal); Investigation (equal). **M. Drillon**: Formal analysis (equal); Investigation (equal); Supervision (equal); Writing – review & editing (equal). **T. T. Ruan**: Data curation (equal); Formal analysis (equal); Investigation (equal). **S. Schlittenhardt**: Data curation (equal); Formal analysis (equal); Investigation (equal); Writing – review & editing (equal). **M. Ruben**: Supervision (equal); Writing – review & editing (equal). **D. Hagenmüller**: Formal analysis (equal); Investigation (equal); Methodology (equal); Writing – review & editing (equal). **S. Schütz**: Formal analysis (equal); Investigation (equal). **J. Schachenmayer**: Formal analysis (equal); Investigation (equal); Writing – review & editing (equal). **C. Genet**: Investigation (equal); Methodology (equal); Writing – review & editing (equal). **G. Pupillo**: Formal analysis (equal); Funding acquisition (equal); Investigation (equal); Methodology (equal); Supervision (equal); Writing – review & editing (equal). **T. W. Ebbesen**: Conceptualization (equal); Funding acquisition (equal); Investigation (equal); Methodology (equal); Project administration (equal); Writing – original draft (equal); Writing – review & editing (equal).

## DATA AVAILABILITY

The data that support the findings of this study are available from the corresponding authors upon reasonable request.

## REFERENCES

[1] F. J. Garcia-Vidal, C. Ciuti, and T. W. Ebbesen, "Manipulating matter by strong coupling to vacuum fields," Science **373**, eabd0336 (2021).
[2] C. Schäfer, M. Ruggenthaler, H. Appel, and A. Rubio, "Modification of excitation and charge transfer in cavity quantum-electrodynamical chemistry," Proc. Natl. Acad. Sci. U. S. A. **116**, 4883–4892 (2019).
[3] C. Ciuti, G. Bastard, and I. Carusotto, "Quantum vacuum properties of the intersubband cavity polariton field," Phys. Rev. B **72**, 115303 (2005).
[4] E. Orgiu, J. George, J. A. Hutchison, E. Devaux, J. F. Dayen, B. Doudin, F. Stellacci, C. Genet, J. Schachenmayer, C. Genes, G. Pupillo, P. Samori, and T. W. Ebbesen, "Conductivity in organic semiconductors hybridized with the vacuum field," Nat. Mater. **14**, 1123–1129 (2015).
[5] J. Feist and F. J. Garcia-Vidal, "Extraordinary exciton conductance induced by strong coupling," Phys. Rev. Lett. **114**, 196402 (2015).
[6] D. Hagenmüller, J. Schachenmayer, S. Schütz, C. Genes, and G. Pupillo, "Cavity-enhanced transport of charge," Phys. Rev. Lett. **119**, 223601 (2017).
[7] K. Nagarajan, J. George, A. Thomas, E. Devaux, T. Chervy, S. Azzini, K. Joseph, A. Jouaiti, M. W. Hosseini, A. Kumar, C. Genet, N. Bartolo, C. Ciuti, and T. W. Ebbesen, "Conductivity and photoconductivity of a p-type organic semiconductor under ultrastrong coupling," ACS Nano **14**, 10219–10225 (2020).
[8] N. Bartolo and C. Ciuti, "Vacuum-dressed cavity magnetotransport of a two-dimensional electron gas," Phys. Rev. B **98**, 205301 (2018).
[9] G. G. Rozenman, K. Akulov, A. Golombek, and T. Schwartz, "Long-range transport of organic exciton-polaritons revealed by ultrafast microscopy," ACS Photonics **5**, 105–110 (2018).
[10] C. Gonzalez-Ballestero, J. Feist, E. Moreno, and F. J. Garcia-Vidal, "Harvesting excitons through plasmonic strong coupling," Phys. Rev. B **92**, 121402 (2015).
[11] X. Zhong, T. Chervy, L. Zhang, A. Thomas, J. George, C. Genet, J. A. Hutchison, and T. W. Ebbesen, "Energy transfer between spatially separated entangled molecules," Angew. Chem., Int. Ed. **56**, 9034–9038 (2017).
[12] S. Hou, M. Khatoniar, K. Ding, Y. Qu, A. Napolov, V. Menon, and S. Forrest, "Ultralong-range energy transport in a disordered organic semiconductor at room temperature via coherent exciton-polariton propagation," Adv. Mater. **32**, 2002127 (2020).
[13] J. A. Hutchison, T. Schwartz, C. Genet, E. Devaux, and T. W. Ebbesen, "Modifying chemical landscapes by coupling to vacuum fields," Angew. Chem., Int. Ed. **51**, 1592–1596 (2012).
[14] M. A. Sentef, M. Ruggenthaler, and A. Rubio, "Cavity quantum-electrodynamical polaritonically enhanced electron-phonon coupling and its influence on superconductivity," Sci. Adv. **4**, eaau6969 (2018).
[15] A. Thomas *et al.*, "Exploring superconductivity under strong coupling with the vacuum electromagnetic field," arXiv:1911.01459v2 (2019).
[16] A. Thomas, E. Devaux, K. Nagarajan, G. Rogez, M. Seidel, F. Richard, C. Genet, M. Drillon, and T. W. Ebbesen, "Large enhancement of ferromagnetism under a collective strong coupling of YBCO nanoparticles," Nano Lett. **21**, 4365–4370 (2021).
[17] F. Appugliese, J. Enkner, G. L. Paravicini-Bagliani, M. Beck, C. Reichl, W. Wegscheider, G. Scalari, C. Ciuti, and J. Faist, "Breakdown of topological protection by cavity vacuum fields in the integer quantum Hall effect," Science **375**, 1030 (2022).
[18] G. Mazza and A. Georges, "Superradiant quantum materials," Phys. Rev. Lett. **122**, 017401 (2019).
[19] J. Lather, P. Bhatt, A. Thomas, T. W. Ebbesen, and J. George, "Cavity catalysis by cooperative vibrational strong coupling of reactant and solvent molecules," Angew. Chem., Int. Ed. **58**, 10635–10638 (2019).
[20] S. Schutz, J. Schachenmayer, D. Hagenmüller, G. K. Brennen, T. Volz, V. Sandoghdar, T. W. Ebbesen, C. Genes, and G. Pupillo, "Ensemble-Induced strong light-matter coupling of a single quantum emitter," Phys. Rev. Lett. **124**, 113602 (2020).
[21] A. Thomas, J. George, A. Shalabney, M. Dryzhakov, S. J. Varma, J. Moran, T. Chervy, X. Zhong, E. Devaux, C. Genet, J. A. Hutchison, and T. W. Ebbesen, "Ground-state chemical reactivity under vibrational coupling to the vacuum electromagnetic field," Angew. Chem., Int. Ed. **55**, 11462–11466 (2016).
[22] T. E. Li, A. Nitzan, and J. E. Subotnik, "Collective vibrational strong coupling effects on molecular vibrational relaxation and energy transfer: Numerical insights via cavity molecular dynamics simulations," Angew. Chem., Int. Ed. **60**, 15533 (2021).
[23] T. S. Haugland, E. Ronca, E. F. Kjønstad, A. Rubio, and H. Koch, "Coupled cluster theory for molecular polaritons: Changing ground and excited states," Phys. Rev. X **10**, 041043 (2020).
[24] A. Mandal, X. Li, and P. Huo, "Theory of vibrational polariton chemistry in the collective coupling regime," J. Chem. Phys. **156**, 014101 (2022).

[25]T. Fukushima, S. Yoshimitsu, and K. Murakoshi, "Inherent promotion of ionic conductivity via collective vibrational strong coupling of water with the vacuum electromagnetic field," J. Am. Chem. Soc. **144**, 12177 (2022).
[26]A. Thomas, L. Lethuillier-Karl, K. Nagarajan, R. M. A. Vergauwe, J. George, T. Chervy, A. Shalabney, E. Devaux, C. Genet, J. Moran, and T. W. Ebbesen, "Tilting a ground-state reactivity landscape by vibrational strong coupling," Science **363**, 615–619 (2019).
[27]K. Hirai, R. Takeda, J. A. Hutchison, and H. Uji-I, "Modulation of Prins cyclization by vibrational strong coupling," Angew. Chem., Int. Ed. **59**, 5332–5335 (2020).
[28]Y. Pang, A. Thomas, K. Nagarajan, R. M. A. Vergauwe, K. Joseph, B. Patrahau, K. Wang, C. Genet, and T. W. Ebbesen, "On the role of symmetry in vibrational strong coupling: The case of charge-transfer complexation," Angew. Chem., Int. Ed. **59**, 10436–10440 (2020).
[29]W. Ahn, J. F. Triana, F. Recabal, F. Herrera, and B. S. Simpkins, "Modification of ground-state chemical reactivity via light-matter coherence in infrared cavities," Science **380**, 1165 (2023).
[30]M. Balasubrahmaniyam, A. Simkhovich, A. Golombek, G. Sandik, G. Ankonina, and T. Schwartz, "From enhanced diffusion to ultrafast ballistic motion of hybrid light-matter excitations," Nat. Mater. **22**, 338–344 (2023).
[31]S. Kumar, S. Biswas, U. Rashid, K. S. Mony, G. Chandrasekharan, F. Mattiotti, R. M. A. Vergauwe, D. Hagenmuller, V. Kaliginedi, and A. Thomas, "Extraordinary electrical conductance through amorphous nonconducting polymers under vibrational strong coupling," J. Am. Chem. Soc. **146**, 18999 (2024).
[32]F. Schlawin, A. Cavalleri, and D. Jaksch, "Cavity-mediated electron-photon superconductivity," Phys. Rev. Lett. **122**, 133602 (2019).
[33]J. B. Curtis, Z. M. Raines, A. A. Allocca, M. Hafezi, and V. M. Galitski, "Cavity quantum Eliashberg enhancement of superconductivity," Phys. Rev. Lett. **122**, 167002 (2019).
[34]G. M. Andolina, A. De Pasquale, F. M. D. Pellegrino, I. Torre, F. H. L. Koppens, and M. Polini, "Amperean superconductivity cannot be induced by deep subwavelength cavities in a two-dimensional material," Phys. Rev. B **109**, 104513 (2024).
[35]K. Tanigaki, T. W. Ebbesen, S. Saito, J. Mizuki, J. S. Tsai, Y. Kubo, and S. Kuroshima, "Superconductivity at 33 K in $Cs_xRb_yC_{60}$," Nature **352**, 222–223 (1991).
[36]O. Gunnarsson, J. E. Han, E. Koch, and V. H. Crespi, *Superconductivity in Alkali-Doped Fullerides* (Springer Berlin Heidelberg, Berlin, Heidelberg, 2005), pp. 71–101.
[37]A. M. Campbell, F. J. Blunt, J. D. Jonson, and P. A. Freeman, "Quantitative determination of percentage superconductor in a new compound," Cryogenics **31**, 732–737 (1991).
[38]T. Pichler, M. Matus, and H. Kuzmany, "Electron-vibrational mode coupling in $K_3C_{60}$ from IR-transmittance and reflectivity," Solid State Commun. **86**, 221–225 (1993).
[39]T. Pichler, R. Winkler, and H. Kuzmany, "Equilibrium phases in K- and Rb-doped $C_{60}$ from in situ infrared reflectivity measurements," Phys. Rev. B **49**, 15879–15889 (1994).
[40]S. Messelot, C. Symonds, J. Bellessa, J. Tignon, S. Dhillon, J.-B. Brubach, P. Roy, and J. Mangeney, "Tamm cavity in the terahertz spectral range," ACS Photonics **7**, 2906–2914 (2020).
[41]Y. Takabayashi *et al.*, "The disorder-free non-BCS superconductor $Cs_3C_{60}$ emerges from an antiferromagnetic insulator parent state," Science **323**, 1585–1590 (2009).
[42]J. Bardeen, L. N. Cooper, and J. R. Schrieffer, "Theory of superconductivity," Phys. Rev. **108**, 1175–1204 (1957).
[43]W. L. McMillan, "Transition temperature of strong-coupled superconductors," Phys. Rev. **167**, 331–344 (1968).
[44]P. B. Allen and R. C. Dynes, "Transition temperature of strong-coupled superconductors reanalyzed," Phys. Rev. B **12**, 905–922 (1975).
[45]D. Hagenmüller, J. Schachenmayer, C. Genet, T. W. Ebbesen, and G. Pupillo, "Enhancement of the electron-phonon scattering induced by intrinsic surface plasmon-phonon polaritons," ACS Photonics **6**, 1073–1081 (2019).
[46]F. Giustino, "Electron-phonon interactions from first principles," Rev. Mod. Phys. **89**, 015003 (2017).
[47]J. George *et al.*, "Multiple Rabi splittings under ultrastrong vibrational coupling," Phys. Rev. Lett. **117**, 153601 (2016).
[48]M. Mitrano *et al.*, "Possible light-induced superconductivity in $K_3C_{60}$ at high temperature," Nature **530**, 461 (2016).
[49]D. Fausti *et al.*, "Light-induced superconductivity in a stripe-ordered cuprate," Science **331**, 189–191 (2011).